STRATEGIES FOR COMPUTATIONAL EFFICIENCY IN CONTINUUM STRUCTURAL TOPOLOGY OPTIMIZATION

Colby C. Swan and Salam F. Rahmatalla
Center for Computer-Aided Design, University of Iowa, Iowa City, Iowa 52242, USA
E-mail: colby-swan@uiowa.edu, srahmata@engineering.uiowa.edu

Abstract

A methodology of enhanced computational efficiency is presented for continuum topology optimization of sparse structural systems. Such systems are characterized by the structural material occupying only a small fraction of the structure's envelope volume. When modeled within a continuum mechanics and topology optimization framework such structures require models of very high refinement which is computationally very expensive. The methodology presented herein to deal with this issue is based on the idea of starting with a relatively coarse mesh of low refinement and employing a sequence of meshes featuring progressively greater degrees of uniform refinement. One starts by solving for an initial approximation to the final material layout on the coarse mesh. This design is then projected onto the next finer mesh in the sequence, and the material layout optimization process is continued. The material layout design from the second mesh can then be projected onto the third mesh for additional refinement, and so forth. The process terminates when an optimal design of sufficient sparsity, and sufficient mesh resolution is achieved. Within the proposed methodology, additional computational efficiency is realized by using a design-dependent analysis problem reduction technique. As one proceeds toward sparse optimal designs, very large regions of the structural model will be devoid of any structural material and hence can be excluded from the structural analysis problem resulting in great computational efficiency. The validity and performance characteristics of the proposed methodology are demonstrated on three different problems, two involving design of sparse structures for buckling stability, and the third involving design of a hinge-free gripper compliant mechanism.

Introduction

For nearly twenty years, beginning approximately with the work of Bendsøe and Kikuchi (1988), continuum structural topology optimization has been used to investigate optimal forms of structures and mechanical systems. During this time, myriad gains have been realized in understanding how different continuum topology formulations work in relation to an ever-widening circle of applications. Although there are many exceptions, continuum structural topology optimization methods have for the most part been applied to the design of structures and mechanical systems in two-dimensions. One would hope that the methods can eventually be applied to design of structures and mechanical systems in three-dimensions with the same ease that they currently enjoy in two dimensions. If this vision is to become reality, the potentially huge computational costs must be reduced to the extent possible while preserving the inherent generality and flexibility of continuum structural topology optimization. In many design applications, the structural will be very sparse in that the volume of structural material will occupy only a small fraction of the structural system's envelope volume. In such cases, continuum structural topology optimization can require highly refined finite element meshes to achieve convergent and interpretable material layout solutions and models that realistically estimate system performances (i.e. overall compliance; buckling stability; vibrational eigenvalues; etc).

One approach to achieving and dealing with fine meshes in continuum topology optimization [Maute et al. 1998] is to use adaptive mesh refinement to decrease the number of design variables and to seek smooth final topological forms. A similar approach is now extensively involved in finding optimal design forms using the evolutionary structural optimization method (ESO)[3]. In another approach, researchers enforced design symmetry during the optimization process by reducing the design space[4] by, or to remove the void nonstructural elements temporarily from the structural analysis, but reintroduce them if they needed [5,6]. The latter approach has been shown to be very effective in dealing with problems involving geometrical nonlinearity.

M. Pandey et al. (eds), Advances in Engineering Structures, Mechanics & Construction, 673–683.

The material usage constraint is another important factor and plays a considerable role in achieving low weight and certain performances when utilizing continuum topology optimization method. For example, most existing optimal large civil structures such as long span bridges are sparse in nature, where the real structural material occupies only a small percentage (less than 1%) of the structure's envelope volume. Therefore, in utilizing continuum structural topology optimization to obtain optimal design forms for such systems, it is crucial to impose stringent material usage constraint and implement very fine meshes in order to capture a realistic performance for such systems. The importance of such an approach has been demonstrated in a previous work [6] where it proved to be very effective when designing structural systems for buckling instability. Similarly, it has been shown in designing hinge-free compliant mechanisms to achieve considerable flexibility [7], the amount of structural material comprising the mechanism can be progressively reduced until the desired flexibility of the mechanism is achieved. It is also crucial toward this end to use stringent material usage constraint with very fine finite element meshes

This article presents a methodology for solving large-size sparse systems in continuum structural topology design framework based on sequential refinement and size reduction strategy in a new way that is conceptually simple and theoretically sound. In sequential refinement, the proposed methodology solved a preliminary problem involving relatively coarse meshes and moderate material usage constraint. The resulting optimal form from this stage, which comprises the solid structural material, is then mapped onto a finer mesh and with realistic material usage constraint. The new problem is then solved where a new topological form is obtained. The mesh refinement process is repeated until the final design converges to a realistic shape and performance with minimum error.

A size reduction strategy is implemented within each structural analysis, where the void nonstructural elements are removed temporarily from structural analysis but can come back quite easily and naturally if needed. The proposed size reduction technique has been tested on many linear and nonlinear systems involving geometrical nonlinearity and buckling instability and shown to be a very effective and powerful tool for reducing the computational costs, especially when dealing with sparse systems and very fine meshes.

It should be noted here that the current methodology is based on interpolation of nodal design variables using nodal basis functions[8] as opposed to element-based design variables. Although node-based design variables feature C^0 continuity, they must generally be used with perimeter constraints to achieve design convergence with mesh refinement.

Problem Formulations

Structural Model and Material Layout Description

The objective of continuum structural optimization is to find a layout of a structural material of specified properties in a defined spatial region that provides optimum structural performance. In order that the widest possible class of structural layouts can be considered, the methods in question must accommodate such generality. In this work, the spatial region that the candidate structural models can occupy is denoted Ω_s. To facilitate both description of the structural material layout in Ω_s and analysis of the performance associated with each layout considered, the domain is discretized into a relatively fine mesh of nodes and finite elements.

It is desired that at the end of the form-finding process, the structural region Ω_s will be decomposed into a collection of regions cumulatively denoted Ω_A that contain the structural material in question, and the remaining regions $\Omega_B = \Omega_s \setminus \Omega_A$ that are devoid of structural material. Since solution of the form-finding problem in this way is ill-posed, an alternative relaxed approach is usually employed, wherein it is assumed that an amorphous "mixture" of structural material A and a void material B exists throughout the structural region Ω_s. In each region of Ω_s, the nature of the mixture is characterized by a local volumetric density ϕ_A of structural material A. By permitting mixtures, the structural material A and a fictitious void material B are allowed to simultaneously occupy an infinitesimal neighborhood about each Lagrangian point $\mathbf{X} \in \Omega_s$. The volumetric density of structural material A at a fixed Lagrangian

point $\mathbf{X} \in \Omega_s$ is denoted by $\phi_A(X)$ and represents the fraction of an infinitesimal region surrounding point **X** occupied by material A. Natural constraints upon the volumetric densities are:

$$0 \le \phi_A(\mathrm{X}) \le 1; \qquad 0 \le \phi_B(\mathrm{X}) \le 1; \qquad \phi_A(\mathrm{X}) + \phi_B(\mathrm{X}) = 1. \tag{1}$$

Clearly, when $\phi_A(X) = 1$ the point **X** contains solid structural material, and when $\phi_A(X) = 0$ the point **X** is devoid of structural material. The last physical constraint of (1) states that the material volume fractions at **X** are not independent and so one need only be concerned with the layout of structural material A. The design of a structure is here considered to be the spatial distribution of the structural material A in Ω_s.

To describe the distribution of material A throughout Ω_s using a finite number of design parameters, the volumetric density at each of the NUMNP nodal point forms a set of NUMNP design variables. These are then interpolated over the space of all intermediate points in the structure using the nodal shape functions:

$$\varphi(\mathbf{X}) = \sum_{i=1}^{\mathrm{NUMNP}} b_i N_i(\mathbf{X}) \qquad \forall\, \mathbf{X} \in \Omega_s \tag{2}$$

where b_i are the nodal volumetric density values associated with the structural material; and $N_i(\mathbf{X})$ are the nodal shape functions. This approach yields a C^0 continuous design variable field that is not susceptible to "checkerboarding" instabilities.

Given the finite element model of the structural region Ω_s, the structural loads and restraints (or supports) on this region are specified as the set of design loads. For each set of design loadings, and for each realization of the design vector $\mathbf{b} = \{b_1, b_2, \mathrm{K}, b_{NUMNP}\}$, the response performance of the structure will be analyzed as a boundary value problem. From the computed response of the structure, the performance of the structure will be quantified, as will be the sensitivity of the performance to variations in the design variables.

Constitutive Mixing Rules

In the proposed design framework, each finite element comprising the spatial domain Ω_s of the structure will generally contain a spatially varying mixture of the structural and void materials. It is necessary to prescribe the stiffness (or elastic moduli) of such mixtures in terms of the stiffness characteristics of the solid material $\mathbf{C}_{\text{solid}}$, those of the fictitious void material $\mathbf{C}_{\text{void}}$, and the local volumetric density of the structural material $\varphi(\mathbf{X})$. Here, the well-known powerlaw formula (Bendsøe and Sigmund 1999) is used to accomplish this task, providing the local effective stiffness of the mixture $\mathbf{C}^*$ as:

$$\mathbf{C}^* = \varphi^p \mathbf{C}_{\text{solid}} + (1 - \varphi^p)\mathbf{C}_{\text{void}} \tag{3}$$

where typically the mixing rule parameter $p \in [1,4]$. With p=1, the Voigt rule of mixtures is obtained which does not penalize mixtures, but which does yield a convex formulation for compliance minimization problems (Swan and Kosaka, 1997) so that only one solution exists for the design problem. With p=4, mixtures are penalized in the final design, so that regions of Ωs tend to be either solid or void, but the optimization problem is not convex, and will admit a number of solutions that satisfy the first order optimality conditions.

Structural Analysis

For each design, a structural analysis problem is solved on the continuum domain Ω_s. In general terms, the structural analysis problem solved for each realization of the design vector **b** is the following: Find the displacement field $\mathbf{u}(\mathbf{X})$ $\Omega_s \rightarrow \Re^3$ such that the variational equilibrium problem is solved:

$$\int_{\Omega_s} \boldsymbol{\sigma} : \delta\boldsymbol{\varepsilon}\, d\Omega_s = \int_{\Gamma_s} \mathbf{h} \cdot \delta\mathbf{u}\, d\Gamma_s + \int_{\Omega_s} \rho\mathbf{g} \cdot \delta\mathbf{u}\, d\Omega_s \tag{4}$$

where $\boldsymbol{\sigma}(\mathbf{X})$ is the local stress field in the structure; $\mathbf{h}$ is a traction vector consistent with the design loads being applied to the structure; $\rho(\mathbf{X})$ is the local mass density of the structural material; $\mathbf{g}$ is the gravitational body force vector; $\delta\mathbf{u}$ is a kinematically admissible variational displacement field; and $\delta\boldsymbol{\varepsilon}$ is the corresponding variational strain field. In the structural model, the material features linear elastic behavior such that $\boldsymbol{\sigma} = \mathbf{C}^* : \boldsymbol{\varepsilon}$ where the effective elasticity tensor is design dependent and prescribed in accordance with Eq. (3). The matrix problem associated with variational equilibrium of the discrete finite element structural model, for which $\mathbf{u}(\mathbf{X}) = \sum_i N_i(\mathbf{X})\,\mathbf{u}_i$, is

$$\mathbf{0} = \mathbf{K}\cdot\mathbf{u} - \mathbf{f}^{\text{ext}} = \mathbf{f}^{\text{int}} - \mathbf{f}^{\text{ext}} \tag{5}$$

where:

$$\begin{aligned} \mathrm{K}_{jk}^{LM} &= \int_{\Omega_s} \mathrm{B}_{mj}^{L}\,\mathrm{C}^*_{\mathrm{mn}}\,\mathrm{B}_{\mathrm{nk}}^{\mathrm{M}}\,\mathrm{d}\Omega_{\mathrm{s}} \\ \mathbf{f}^{\text{int}} &= \mathbf{K}\cdot\mathbf{u} = \int_{\Omega_s} \mathbf{B}^T\boldsymbol{\sigma}\,\mathrm{d}\Omega_{\mathrm{s}} \\ \mathbf{f}^{ext} &= \int_{\Gamma_s} N\,\mathbf{h}\,\mathrm{d}\Gamma_{\mathrm{s}} + \int_{\Omega_s} N\,\rho\mathbf{g}\,\mathrm{d}\Omega_{s}. \end{aligned} \tag{6}$$

In all of the above, N denote the nodal shape functions and $\mathbf{B}$ denote the standard strain-displacement matrices [*c.f.* Bathe, 1996]. The structural stiffness matrix $\mathbf{K}$ is positive definite due to the characteristics of the effective elasticity tensor $\mathbf{C}^*$, and this guarantees a unique solution to the structural analysis problem for each realization of the design $\mathbf{b}$.

Once the equilibrium solution to the problem of Eq. (5) is obtained, then the linearized geometrical stiffness matrix $\mathbf{G}$ can be computed based on the stress field $\boldsymbol{\sigma}$ in the structure:

$$G_{jk}^{LM} = \int_{\Omega_s} N_{,m}^{L}\,N_{,n}^{M}\,\sigma_{\mathrm{mn}}\delta_{jk}\,d\Omega_s \tag{7}$$

It is worth noting that G is not necessarily positive definite but rather depends heavily upon the nature of the stress field in the structure. A purely tensile stress field clearly makes G positive definite, although for any compressive stresses, G will not be positive definite.

Structural Performance Measures

As noted previously, structural topology design problems can be formulated in a number of alternative ways through utilization of assorted objective and constraint functions. Generally, the objective function measures the performance of the structure, and the constraint function limits the amount of structural material that can be used, although the roles can be reversed equally well. The significant aspects of using CSTO to design large-scale sparse structures can be demonstrated here using the linear elastic structural compliance performance measure and the critical load buckling factor.

Linear Elastic Structural Compliance

If a structure features a linear elastic response behavior, the resulting displacement field $\mathbf{u}$ in response to a set of applied external loads $\mathbf{f}^{ext}$ will be simply $\mathbf{u} = \mathbf{K}^{-1}\cdot\mathbf{f}^{\text{ext}}$ where $\mathbf{K}$ represents the stiffness matrix of the structure. For a given set of loads, the compliance $\Pi(\mathbf{b})$ of the structure is simply

$$\Pi(\mathbf{b}) = \frac{1}{2}\mathbf{f}^{\text{ext}}\cdot\mathbf{u}\ . \tag{8}$$

Structural concept designs $\mathbf{b}$ that are stiff with respect to the applied loads will have small compliance $\Pi(\mathbf{b})$, whereas structures that are not stiff with respect to the applied loads will have large compliance. To facilitate usage of gradient-based optimization solution techniques, it is necessary to compute the design derivatives of the compliance function. It can be shown that the design gradient of structural compliance is provided by the following expression:

$$\frac{d\Pi}{d\mathbf{b}} = -\frac{1}{2}\mathbf{u}\cdot\left(\frac{\partial \mathbf{K}}{\partial \mathbf{b}}\cdot\mathbf{u} - \frac{\partial \mathbf{f}^{\text{ext}}}{\partial \mathbf{b}}\right) \tag{9}$$

Linearized Buckling Performance Measure

Linearized buckling eigenvalue analysis proceeds as follows: A prescribed force loading $\mathbf{f}^{\text{ext}}$ is applied to the structure with its magnitude necessarily being less than that required to induce geometric instability in the structure. Once the resulting linear, elastostatic displacement solution $\mathbf{u} = \{u_i\} \in \boldsymbol{R}^N$ in response to the applied loading $\mathbf{f}^{\text{ext}}$ is obtained $\left(\mathbf{K}\cdot\mathbf{u} = \mathbf{f}^{\text{ext}}\right)$, where $\mathbf{K}$ is the linearized stiffness matrix, then the following eigenvalue problem is solved

$$\left[\mathbf{K}(\mathbf{b}) + \lambda\mathbf{G}(\mathbf{u},\mathbf{b})\right]\cdot\boldsymbol{\psi} = \mathbf{0} \tag{10}$$

In the preceding, $\mathbf{b} = \{\mathbf{b}_e\} \in \boldsymbol{R}^M$ is again the vector of design variables; $\mathbf{K}$ is the tangent stiffness operator; $\mathbf{G}(\mathbf{u},\mathbf{b})$ is the linearized geometric stiffness matrix; $\lambda = -(\boldsymbol{\psi}\cdot\mathbf{K}\cdot\boldsymbol{\psi})/(\boldsymbol{\psi}\cdot\mathbf{G}\cdot\boldsymbol{\psi})$ is an eigenvalue denoting the magnitude by which $\mathbf{f}^{\text{ext}}$ must be scaled to create instability in the structure, and $\boldsymbol{\psi}$ is a normalized eigenvector satisfying $\boldsymbol{\psi}\cdot\mathbf{K}\cdot\boldsymbol{\psi} = 1$. To avoid numerical difficulties in the solution of (10) stemming from the indefinite characteristics of $\mathbf{G}$, it is common (Bathe 1996) to solve a modified eigenvalue problem that deals with two positive definite matrices.

$$\left[(\mathbf{K}+\mathbf{G}) - \gamma\,\mathbf{K}\right]\cdot\boldsymbol{\psi} = \mathbf{0} \tag{11}$$

where

$$\gamma = \frac{\lambda - 1}{\lambda} \Leftrightarrow \lambda = \frac{1}{1-\gamma}. \tag{12}$$

In Eq. (11), the matrix **K** is positive definite irrespective of the loading applied to the structure, whereas the matrix (**K**+**G**) will only be positive definite when the magnitude of the loading applied to the structural model is less than the critical magnitude that creates instability in accordance with linearized buckling theory.

The design problem is formulated to maximize the calculated minimum-buckling load factor (λ), and accordingly the objective function f_E to be minimized for this problem would simply be the reciprocal of the lowest eigenvalue λ as follows.

$$f_E(\mathbf{u},\mathbf{b}) = \frac{1}{\min(\lambda)} \tag{13}$$

The optimization problem is thus stated to minimize the reciprocal of the first (or minimum) critical buckling load as follows

$$\min_{\mathbf{b},\mathbf{u}} f_E = \min_{\mathbf{b},\mathbf{u}}\left(\frac{1}{\lambda}\right) = \min_{\mathbf{b},\mathbf{u}}\left(-\max_{\|\boldsymbol{\psi}\|\neq 0}\frac{\boldsymbol{\psi}\cdot\mathbf{G}\cdot\boldsymbol{\psi}}{\boldsymbol{\psi}\cdot\mathbf{K}\cdot\boldsymbol{\psi}}\right) \tag{14}$$

subject to the normal bound constraints on the design variables (1), the linear structural equilibrium state equation (5), and a constraint on material resources.

The design gradient of the objective function can be expressed as:

$$\frac{\mathrm{d}f_E}{\mathrm{d}\mathbf{b}} = \frac{\partial f_E}{\partial \mathbf{b}} + \frac{\partial f_E}{\partial \mathbf{u}}\cdot\frac{\partial \mathbf{u}}{\partial \mathbf{b}} \tag{15}$$

To avoid explicit computation of the term $\frac{\partial \mathbf{u}}{\partial \mathbf{b}}$, adjoint design sensitivity analysis is employed by augmenting the objective function f_E with the equilibrium state equation as follows

$$\Xi = f_E + \mathbf{u}^a\cdot\mathbf{r} \tag{16}$$

where $\mathbf{u}^a$ is the adjoint displacement vector which functions as a matrix of Lagrange multipliers and determined by the solution of a linear adjoint problem. The design derivative of the augmented Lagrangian is then written as follows:

$$\frac{\mathrm{d}\Xi}{\mathrm{d}\mathbf{b}} = \left(\frac{\partial f_E}{\partial \mathbf{b}} + \mathbf{u}^a \cdot \frac{\partial \mathbf{r}}{\partial \mathbf{b}} \right) + \left[\frac{\partial f_E}{\partial \mathbf{u}} + \frac{\partial \mathbf{r}}{\partial \mathbf{u}} \cdot \mathbf{u}^a \right] \cdot \frac{\partial \mathbf{u}}{\partial \mathbf{b}} + \left(\mathbf{r} \cdot \frac{\partial \mathbf{u}^a}{\partial \mathbf{b}} \right) \tag{17}$$

The last term of Eq. (17) vanishes due to satisfaction of the equilibrium constraint ($\mathbf{r}=\mathbf{0}$), and the second term can be made to vanish by selecting the adjoint displacement vector to solve the following linear adjoint equality statement

$$\mathbf{K} \cdot \mathbf{u}^a = \boldsymbol{\psi} \cdot \frac{\partial \mathbf{G}}{\partial \mathbf{u}} \cdot \boldsymbol{\psi} \,. \tag{18}$$

Since it can be shown that $\mathrm{d}\Xi / \mathrm{d}\mathbf{b} = \mathrm{d}f_E / \mathrm{d}\mathbf{b}$, it follows that the design gradient expression for the objective function is

$$\frac{\mathrm{d}f_E}{\mathrm{d}\mathbf{b}} = -\boldsymbol{\psi} \cdot \left(\frac{\partial \mathbf{G}}{\partial \mathbf{b}} + \frac{1}{\lambda} \frac{\partial \mathbf{K}}{\partial \mathbf{b}} \right) \cdot \boldsymbol{\psi} + \mathbf{u}^a \cdot \left(\frac{\partial \mathbf{K}}{\partial \mathbf{b}} \cdot \mathbf{u} - \frac{\partial \mathbf{f}^{ext}}{\partial \mathbf{b}} \right). \tag{19}$$

The preceding expression is valid only when the minimum eigenvalue is a simple, or non-repeated, eigenvalue. When the minimum eigenvalue is nonsimple, or repeated, the variation of the eigenvalue in design space is non-smooth, and direct usage of the expression in Eq. (19) is technically incorrect (Choi et al 1983; Seyranian *et al* 1994). Resolution of this issue is nontrivial, although it can be ameliorated somewhat by using small and variable move limits in the design optimization process. Despite this challenge, designs that successfully maximize the buckling stability of a structural system can nevertheless be obtained. Further details on formulation and solution of stability design problems using linearized buckling theory are provided in Rahmatalla and Swan[10].

Analysis Problem Size Reduction Technique

In continuum topology optimization of sparse structures with limited structural material usage and realistically large design loads, geometrical instabilities become a definite possibility. If modeled, geometrical instabilities in structural systems can result in finite deformations. The modeling of finite deformations in mixed solid-void grid-like meshes used in continuum structural topology optimization can result in excessive distortion of void or low-density elements that can in turn lead to numerical difficulties solving the structural analysis problem. Since the optimization process in continuum topology optimization typically removes structural material from low stress, or low-sensitivity areas, fairly substantial regions of low-density elements are common. As these elements are highly compliant, they contribute very little to structural stability, while being subject to excessive deformation that creates numerical difficulties. Therefore, it is sometimes advantageous to identify these large regions of void and low-density elements and to remove them, at least temporarily, from the structural analysis problem. An automated algorithm for identifying such regions and removing them from the structural analysis problem is presented and discussed below. It is worth noting that the procedure proposed and investigated here is reversible in that it permits low-density regions of the structure to return as high-density structural regions even after they have previously been removed from consideration during structural analysis.

The essence of the proposed analysis problem reduction technique can be captured in the three steps listed below:

1. All finite elements in the structural analysis model that are devoid of solid material, or nearly so, are identified as “void” elements. (Typically, in the examples presented below, if an element’s volume fraction of solid material is less than or equal to .002, it is identified as “void”.)

2. All nodes that are members only of "void" elements are identified as "prime" nodes. The degrees of freedom of such "prime" nodes are restrained, reducing the size of the analysis problem.
3. If only "prime" nodes comprise an element, that element is then denoted as a "prime" element. Such "prime" elements are then neglected in the structural analysis problem so that if they undergo excessive distortion it does not create any singularities in the system of finite element equations. It is worth noting, that "prime" elements are those that are surrounded by "void" elements.

A graphical description supporting the explanation of this technique for reducing the analysis problem is presented in Figure 1.

The matter of reducing the analysis problem by neglecting significant regions of void elements has been addressed in preceding works [9,10]. The current reduction techniques have proven to be both robust and efficient in all of the example problems presented in the section below. The techniques are especially powerful and effective when applied in design problems involving extremely sparse structures, since highly refined meshes are needed when very stringent material resource constraints are imposed. When a fine mesh is employed with a very limited amount of structural material, the proposed reduction techniques will allow for dramatic savings in computing effort.

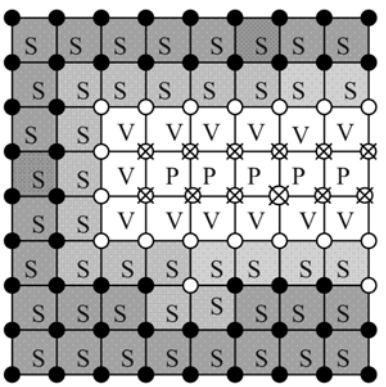

Figure 1. Schematic of partial mesh to illustrate analysis problem reduction technique. Nodes having vanishing design variable values are denoted with open circles; filled circles denote nodes associated with nonzero design values; nodes represented by open circles with X's are "prime" nodes whose degrees of freedom are restrained in the size reduction method. Elements designated with "S" are at least partially solid and those with "V" are devoid of material. Those designated with "P" are prime and need not be considered during structural analysis since all of their degrees of freedom are restrained.

Examples

The validity of the proposed methodology is demonstrated in this article on three problems,where the first two are benchmark linear stability design problems with extreme sparsity and the third involves design of a very sparse, hinge-free gripper compliant mechanism. In all problems presented, the void material is assumed to have a stiffness equal to that of structural material scaled down by a factor of 10^{-6}.

Stability Design of Sparse Structure under Fixed-Fixed End Conditions

In this problem, a point load is applied to the top central portion of a structural region with fixed supports at both lateral edges of the domain. A sparse, stable structural design is sought that carries the applied load back to the supports. This problem is solved here by optimizing the material layout such that the minimum buckling eigenvalue is maximized. Details on the formulation of such problems were presented in references 6 and 8. The problem has also been solved using different formulations and objective functions by Buhl *et al* (2000) and Gea and Luo (2001). In this specific example (Figure 2a), a point load of magnitude $1.0 \cdot 10^5$ is applied to the domain as shown which has relative dimensions of 100 by 50. The optimization problem is solved to find the constrained material layout under the applied loading that maximizes the minimum buckling eigenvalue (see Eq. 14).

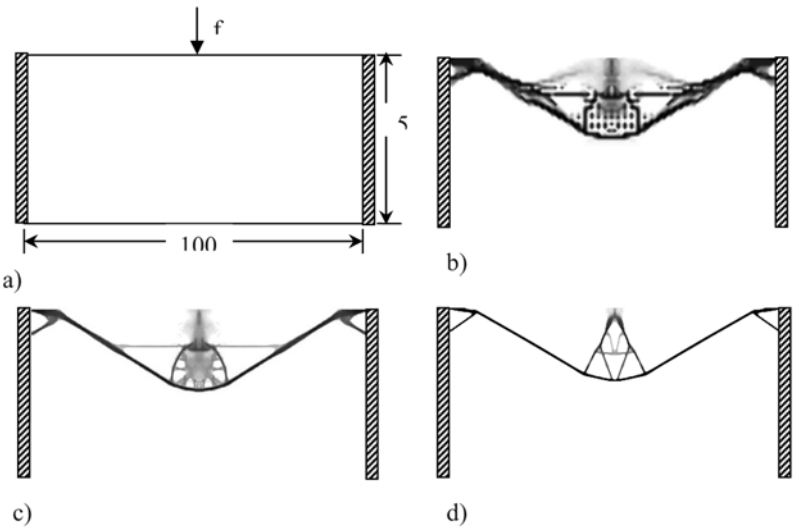

Fig. 2. Stability design of sparse structure for fixed-fixed end conditions. a) shows the design domain, support conditions, and loading; b) design obtained on a mesh of 100 x 50 bilinear elements with material usage constraint of 0.10; b) preceding design mapped onto mesh of 200 x 100 elements and further optimized while imposing a tightened material usage constraint of 0.05, and a perimeter constraint of 5000; d) preceding design mapped onto mesh of 400 x 200 elements and further optimized with material usage constraint of 0.03 and perimeter constraint of 3750.

The material layout optimization problem was first solved on a relatively coarse mesh of 100 by 50 bilinear quadrilateral continuum elements. The material layout shown in Figure 2b was obtained from a starting "design" of structural material completely occupying the entire the structural region, followed by imposition of a constraint on structural material: $V_{material} \leq 0.20 V_{domain}$ where V_{domain} represents the volume of the 100 by 50 structural domain. The design solution shown was obtained using a powerlaw parameter [p=1.75]. The material layout in Fig. 2b is both heavy and somewhat difficult to interpret. Consequently, the design shown was then projected onto a uniformly refined mesh of 200 by 100 bilinear continuum elements. With this refine mesh, a reduced material usage constraint of $V_{material} \leq 0.080 V_{domain}$ was imposed in addition to a perimeter constraint $P \leq \frac{1}{2}(l+h)$ where l and h are the lateral and vertical dimensions of the structural region in Fig. 2a. The material layout was then optimized on the refined mesh for 100 SLP (sequential linear programming) iterations with the result being as shown in Fig. 2c. To obtain a very clear, yet sparse, structural design, the design of Fig. 2c. was then mapped onto a mesh of 400 by 200 bilinear continuum elements. The material usage constraint was tightened to $V_{material} \leq 0.030 V_{domain}$, and a mixing rule powerlaw parameter of [p=4] was employed along with a tightened perimeter constraint $P \leq \frac{1}{3}(l+h)$. The final, optimal material layout design achieved is as shown in Fig. 2d. This final design shown in Fig. 2d. is similar those obtained in the previous study by the authors using this same problem[6].

Circular Domain Stability Design Problem

In this second test problem, the circle domain test problem introduced previously by the authors (Rahmatalla and Swan, 2003, 2004) is revisited. A downward acting point-load of magnitude $1.0 \cdot 10^9$ is applied at the center-node of the circular structural domain of radius R=50. In Fig. 3a, the coarsest mesh features 896 bilinear elements; the next mesh (3c) features 3584 elements; that of (3e) features 14,336 elements; and the finest (3g) features 57,344 elements. The design objective is to find the optimal form of

structure that carries the design from the center back to the fixed boundaries. The design problem was first solved on the coarse mesh of 896 elements with a powerlaw value [p=1.75] and a material usage constraint $V_{material}/V_{structure} \leq 0.20$ and the resulting design is shown in Fig. 3b. This design was then mapped onto the mesh of Fig.3c and the layout optimization continued with [p=2.5] with a tightened material usage constraint of $V_{material}/V_{structure} \leq 0.05$. The resulting design (Fig. 3d) was then projected onto the mesh of (Fig. 3e), and the optimization process continued with [p=4.0] and an even tighter material usage constraint of $V_{material}/V_{structure} \leq 0.015$. The design obtained from Fig. 3f. was projected onto the finest mesh and further optimized with the same powerlaw value and material usage constraint. The buckling eigenvalue on the finest mesh and the material layout are in close agreement with those from the previous mesh, and in this sense have converged.

Size reduction was essential to these computations. As the refinement process utilized finer and finer meshes, the analysis problem size remained very modest in size. For example, even on the finest mesh of 57,344 elements, the reduced problem size involved only 4,464 degrees of freedom, and the actual structural and eigenvalue analysis were performed on an HP J-class workstation in less than 10 cpu-seconds.

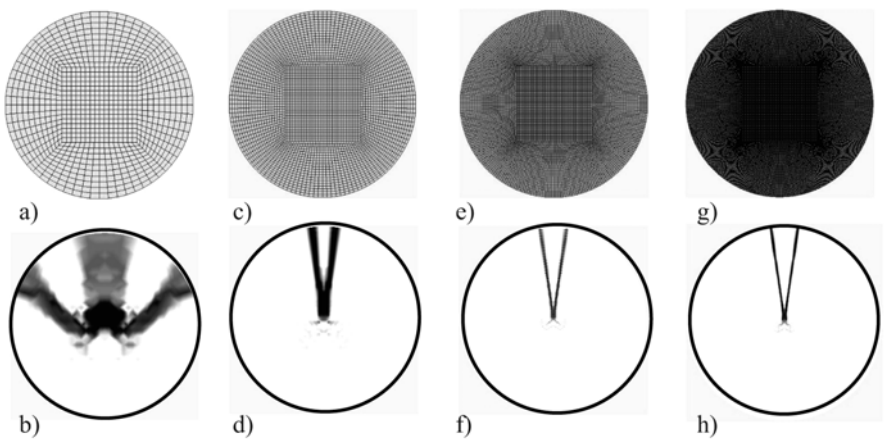

Figure 3. a) coarsest mesh of 896 elements; b) design with $V_{mat}/V_{structure}$ =0.20 and $\lambda=2.17\cdot10^{3}$; c) mesh with 3,584 elements; d) material layout design with $V_{mat}/V_{structure}$ =0.05 and $\lambda=1.20\cdot10^{2}$; e) mesh with 14,336 elements; f) material layout design with $V_{mat}/V_{structure}$ =0.015 and $\lambda=1.00\cdot10^{1}$; g) mesh with 57,344 elements; h) material layout design with $V_{mat}/V_{structure}$ =0.015 and $\lambda=1.05\cdot10^{1}$;

Sparse Compliant Mechanism Design Problem

In this final example, the importance of the proposed methodology is explored by considering the design of hinge-free gripper mechanism [7]. The design domain for this problem is shown in Fig. 4a. When a horizontal force is applied at the input port, the opposing output ports move vertically to pinch and thus grip a workpiece. The mechanism is designed with aluminum. In the first stage, the mechanism is designed utilizing a quadrilateral bilinear mesh of 5,000 elements and a material usage constraint of 12%. The resulting topology depicted in Fig.4b looks reasonable with no hinges in the resulting design; yet, such design is very stiff and very hard to use. Accordingly, a better design with higher flexibility can be achieved by using less material usage constraint; in this case, the material usage constraint is set at 3%. In order to capture a realistic performance with such a sparse system, the resulting topology is mapped onto a finer mesh of 22,500 elements and the resulting topology is shown in Fig.4c. In spite of this relatively fine mesh, it is still not capable of handling such a sparse system; therefore, it is very important to use a finer mesh. Thus, the resulting topology is then mapped onto a mesh of 90,000 elements, and the material usage constraint is kept at the same level of 3%; the resulting topology is shown in Fig. 4d. While this

resulting topology looks much better and clearer than the previous one, more refinement is still needed in order to achieve a final design.

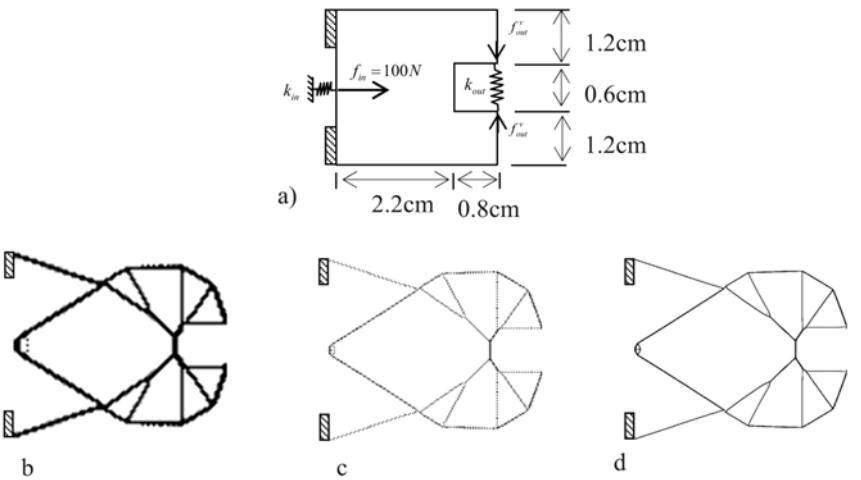

Figure 4. The gripper mechanism. a) the design domain and loading conditions; b) the resulting topology utilizing 5,000 quadrilateral bilinear elements with 12% material usage constraint; c) the resulting topology utilizing 22,500 finite elements and 3% material usage constraint; d) the resulting topology utilizing 90,000 elements and 3% material usage constraint.

Summary

In this work, a new methodology is introduced to solve large-size sparse systems in continuum topology optimization framework with relatively very low computational costs. The validity and performance of the proposed methodology has been demonstrated here in two examples involving linear and compliant mechanism design problems; however, the methodology has been successfully tested on numerous problems involving geometrical nonlinearity and buckling stability.

References

Bendsoe, M.P.; Kikuchi, N. 1988: Generating optimal topology in structural design using a homogenization method, *Comput. Meth. Appl. Mech. Engng*, 71, 197-224.

Bendsøe, M.P.; Sigmund, O. 1999: Material interpolations in topology optimization. *Archive of Applied Mechanics*, 69, 635-54.

Bruns, T. E.; Tortorelli, D. A. 2003: An element removal and reintroduction strategy for the topology optimization of structures and compliant mechanisms, *Int. J. Num. Meth. Engng*, 57(10), 1413-1430.

Buhl, T.; Pedersen, W.; Sigmund, O. 2000: Stiffness design of geometrically nonlinear structures using topology optimization, *Struct. Multidisc. Optim*., 19, 93-104.

Bulman, S.; Sienz, J.; Hinton, E. 2001: Comparison between algorithms for structural topology optimization using a series of benchmark studies*, Computers and Structures*, 79(12), 1203-18.

Gea, H. C.; Luo, J. 2001: Topology optimization of structures with geometrical nonlinearities, *Computers and Structures*, 79, 1977-85.

Haber, R.B.; Jog, C.S.; Bendsøe, M.P. 1996: A new approach to variable-topology shape design using a constraint on perimeter. *Struct. Optim.* 11, 1–12.

Kosaka, I.; Swan, C.C. 1999: A symmetry reduction method for continuum structural topology optimization. *Computers and Structures*, 70(1), 47-61

Maute, K.; Schwarz, S.; Ramm, E. 1998: Adaptive topology optimization of elastoplastic structures, *Struct. Optim*. 15, 81-91.

Michell, A.G.M. 1904: The limits of economy in frame structures. *Philosophical Magazine* Sect. 6, 8(47), 589-597.

Rahmatalla, S.; Swan, C.C. 2003: Continuum topology optimization of buckling-sensitive structures, *AIAA J*. 41(5), 1180-1189.

Rahmatalla, S.; Swan, C.C. 2003: Form-finding of sparse structures using continuum topology optimization. *J. Struct. Engng.* 129(12), 1707-16.

Rahmatalla, S.; Swan, C.C. 2004: A Q4/Q4 continuum structural topology optimization implementation. *Struct. Multidis. Optim.* 27, 130-135.

Rahmatalla, S.F.; Swan, C.C., 2005: Sparse monolithic compliant mechanisms using continuum structural topology optimization, *Int. J. Num. Meth. Engng*.

Swan, C.C.; Kosaka, I. 1997: Voigt-Reuss topology optimization for structures with nonlinear material behaviors, *Int. J. Numer. Meth. Engng*., 40, 3785-814.